PHYSICAL REVIEW D VOLUME 40, NUMBER 7 1 OCTOBER 1989

Roper resonance and the baryon spectrum

J. A. Elsey and I. R. Afnan
School of Physical Sciences, The Flinders University of South Australia, Bedford Park, South Australia 5042, Australia
(Received 29 December 1988)

We present a method for calculating the baryon spectrum in the cloudy-bag model in which the masses of the baryons are identical to the poles of the S matrix in the complex energy plane. In particular, we demonstrate that the width for the decay of these resonances by pion emission is dependent on whether the calculations are carried out on the real energy axis or at the resonance poles, the latter being consistent with the scattering experiments that determine these widths. Results for $N^*(1440)$ are presented.

I. INTRODUCTION

Quarks and gluons are well established as being the constituents of nuclei and their dynamics are described by quantum chromodynamics (QCD). As a result, one would like to describe nuclei using these constituents as a starting point, but the complexity of the QCD equations renders this a very difficult problem. Consequently the nuclear physicist has relied on phenomenological models which try to emulate QCD by incorporating its most important properties.

Bag models[1] have been used quite successfully to achieve this goal. They picture the quarks in the hadron as being confined to a static volume, the bag. The important QCD properties of asymptotic freedom[2] and infrared slavery[3] are included by neglecting the quark interaction via the exchange of gluons to lowest order and by imposing appropriate boundary conditions at the bag surface. The earliest of these models was the MIT bag model[4] which was covariant and based on a field-theoretic Lagrangian. Its main shortcoming was its failure to satisfy chiral symmetry,[5] which is one of the fundamental symmetries of QCD. The restoration of chiral symmetry has been achieved by coupling a pion field to the bag. The first chirally symmetric bag was proposed by Chodos and Thorn,[6] and this was followed by the chiral bag model of Brown and Rho.[7] There have been other chiral bag models since the Brown-Rho model. One that has been extensively used for π-N scattering is the cloudy-bag model (CBM) of Théberge, Thomas, and Miller.[8] Although our formalism does not depend on any particular model, we used the CBM with pseudosocalar coupling of the pion field to the quarks at the bag surface[1] to obtain some numerical results.

It has become a standard practice to test any model of QCD by calculating the baryon spectrum. Considering the fact that many of the states in the baryon spectrum are observed as resonances in meson-nucleon scattering, i.e., they correspond to poles of the corresponding S matrix in the complex energy plane, it is surprising that the calculation of the baryon spectrum is often carried out as a bound-state problem. In fact, some of these models calculate the mass and width of the states using different Lagrangians, when these quantities are nothing more than the real and imaginary parts of the energy at which the S matrix has a pole. Here we will show how we can calculate the baryon spectrum as an eigenvalue problem for a complex Hamiltonian, with the imaginary part of the Hamiltonian giving the mechanism for the decay of the state by meson emission. Although the derivation of our final result can be achieved in a covariant manner by the classification of diagrams according to their irreducibility,[9] we have chosen to use Feshbach projection operators[10] to demonstrate how the coupling between the different channels gives the mass shift and width of the states in the spectrum. Furthermore we show that the complex eigenvalues resulting from the diagonalization of the complex Hamiltonian are the positions of the poles of the S matrix for meson-nucleon scattering. This formulation is presented in Sec. II.

To demonstrate our formalism we have considered the Roper resonance, i.e., $N^*(1440)$, within the framework of CBM as a radial excitation of the nucleon. The motivation for this choice is twofold. (i) This model has been used to calculate the π-N phase shift in this channel, always resulting in a resonance with a width that is substantially smaller than experiment.[11,12] On the other hand, the determination of the mass and width of this resonance, in the CBM and in the spirit of mass spectrum calculation, gives rise to good agreement between theory and experiment.[13] This suggests an inconsistency between the two methods, since both approaches are based on the same CBM Lagrangian. (ii) It has been suggested that the recent phase-shift analysis in the energy region of the Roper resonance can be interpreted in terms of two poles in the complex energy plane.[14,15] This implies that the Roper resonance might be two overlapping resonances. The bag model predicts two states corresponding to the [56] (spatially symmetric) and the [70] (spatially mixed symmetry) representation of SU(6). By including both of these states, we will see how the mixing between the two states leads to two physical resonances in the P_{11} channel, and how the two poles affect the phase shifts. We will also be able to give the relative contribution of the two states to each of the two resonances. This is particularly important since many of the phase-shift calcula-

tions[11,12,16] have included the [56] representation only.

In Sec. III, we present our results for the resonances in the P_{11} channel. Here we find that by calculating the baryon states as a complex eigenvalue problem we get a width that is in agreement with the calculated phase shift for the same Lagrangian, and that width is much smaller than what one would get by first calculating the mass of the baryon as a bound-state problem, and then calculating the width. This discrepancy between the two methods raises a question regarding the accuracy of any calculation of the baryon spectrum which gives the mass of the baryon as the eigenvalue of a real Hamiltonian. Furthermore we find that the mixing between the [56] and [70] representation, in general, leads to two resonance poles, the narrower of the two being mainly the [56] representation. This narrow resonance leads to a bump in the phase shift which is the result of a small loop in the Argand plot. Finally, in Sec. IV we present some concluding remarks.

II. FORMULATION OF THE PROBLEM

In this section we demonstrate, using Feshbach projection operators,[10] that the problem of determining the excited baryon spectrum is identical to the evaluation of the position of the poles in the pion-nucleon amplitude in the energy region of the resonance corresponding to a state in the baryon spectrum. In particular we demonstrate that the problem of calculating the baryon spectrum reduces to the determination of the eigenvalues of a complex matrix, the real part of the eigenvalue being the mass of the baryon, while the imaginary part is the width.

For the present analysis we consider Hamiltonians similar in structure to the CBM[1] Hamiltonian, which are of the form

$$H=H_0+H_I\ , \tag{2.1}$$

where H_0 is the kinetic energy of the baryon, $B(B=N,\Delta,R,\ldots)$, and the pion, while H_I has the coupling of the meson to the baryon and is of the form

$$H_I=\sum_{\alpha\beta\mu}\int d\mathbf{p}'d\mathbf{p}\,d\mathbf{k}[f(\mathbf{p},\mathbf{k})a_\alpha^\dagger(\mathbf{p}')a_\beta(\mathbf{p})b_\mu(\mathbf{k}) +\text{H.c.}]\ , \tag{2.2}$$

where α and β label the baryon states, i.e., $\alpha,\beta=N,\Delta,R,\ldots$, while $\mathbf{p}'$ and $\mathbf{p}$ label the corresponding momenta. The pions isospin and momentum are given by μ and $\mathbf{k}$, respectively. Because our baryons are not static, the πBB form factor f is a function of the baryon and pion momenta. The equation we need to solve for the baryon spectrum or for pion-nucleon scattering is of the form

$$H\psi=E\psi\ . \tag{2.3}$$

Because of the form of the interaction Hamiltonian H_I, the states with n pions are coupled to the states of $(n-1)$ and $(n+1)$ pions. Since we are considering pion-nucleon scattering, and because of the coupling between states of different pions, we divide our Hilbert space into three subspaces: (1) P-space which has one baryon and zero pions; (2) Q_1-space which has one baryon and one pion; and (3) Q_2-space which has one baryon and n pions, $n\geq 2$. These are, respectively, characterized by the projection operators

$$P=\sum_\alpha\int d\mathbf{p}|\alpha\mathbf{p}\rangle\langle\alpha\mathbf{p}|\ , \tag{2.4a}$$

$$Q_1=\sum_{\alpha,\mu}\int d\mathbf{p}\,d\mathbf{k}|\alpha\mathbf{p},\mu\mathbf{k}\rangle\langle\alpha\mathbf{p},\mu\mathbf{k}|\ , \tag{2.4b}$$

$$Q_2=\sum_{n=2}^{\infty}\left[\sum_\alpha\sum_{\mu_1,\ldots,\mu_n}\int d\mathbf{p}\,d\mathbf{k}_1\cdots d\mathbf{k}_n|\alpha\mathbf{p},\mu_1\mathbf{k}_1,\ldots,\mu_n\mathbf{k}_n\rangle\langle\alpha\mathbf{p},\mu_1\mathbf{k}_1,\ldots,\mu_n\mathbf{k}_n|\right]\ . \tag{2.4c}$$

Application of these operators to Eq. (2.3), allows us to write three coupled equations of the form

$$(E-H_{PP})P\psi=H_{PQ_1}Q_1\psi\ , \tag{2.5a}$$

$$(E-H_{Q_1Q_1})Q_1\psi=H_{Q_1P}P\psi+H_{Q_1Q_2}Q_2\psi\ , \tag{2.5b}$$

$$(E-H_{Q_2Q_2})Q_2\psi=H_{Q_2Q_1}Q_1\psi\ , \tag{2.5c}$$

where $H_{PP}=PHP$, etc. By eliminating the subspace of $n\geq 2$ pions, we can rewrite the above equations as

$$(E-H_{PP})P\psi=H_{PQ_1}Q_1\psi\ , \tag{2.6a}$$

$$(E-\mathcal{H}_{Q_1Q_1})Q_1\psi=H_{Q_1P}P\psi\ , \tag{2.6b}$$

where

$$\mathcal{H}_{Q_1Q_1}(E)=H_{Q_1Q_1}+H_{Q_1Q_2}\frac{1}{E^+-H_{Q_2Q_2}}H_{Q_2Q_1} =\varepsilon(k)+\omega(k)+v_{\text{eff}}\ . \tag{2.7}$$

Here v_{eff} is an effective interaction which includes the contribution of two or more pions in every intermediate state. The above result follows from the fact that $\langle H_{Q_1Q_1}\rangle=\varepsilon(k)+\omega(k)$, where $\varepsilon(k)=\sqrt{k^2+m_\alpha^2}$ and $\omega(k)=\sqrt{k^2+m_\pi^2}$. Note that here the baryon α is taken to be nonstatic.

To simplify our notation we replace, from this point on, Q_1 by Q. By solving Eq. (2.6a) and substituting into Eq. (2.6b) we obtain

$$\left[E-\mathcal{H}_{QQ}-H_{QP}\frac{1}{E^{+}-H_{PP}}H_{PQ}\right]Q\psi=0 \tag{2.8}$$

whose solution is of the form

$$Q\psi=\phi_Q+G_0T\phi_Q\ . \tag{2.9}$$

In this last expression, ϕ_Q is a plane wave for the pion-baryon system, G_0 is the free propagator

$$G_0(E^{+})=\frac{1}{E^{+}-H_{QQ}}=\frac{\mathcal{P}}{E-H_{QQ}}-i\pi\delta(E-H_{QQ})\ , \tag{2.10}$$

and T is the amplitude for pion-baryon scattering. In Eq. (2.10), $\mathcal{P}$ stands for the principal-value integral. The effective interaction in the Q-space, i.e., Eq. (2.8), is now the sum of two interactions; one gives the contribution due to the coupling to channels with two or more pions, $\mathcal{H}_{QQ}$. The second contribution is due to the coupling to the zero pion channel, i.e., the P channel. Making use of the two-potential theory,[17] we can write the amplitude for pion-baryon scattering as

$$T=t_Q+(t_QG_0+1)H_{QP}\frac{1}{E^{+}-\mathcal{H}_{PP}}H_{PQ}(1+G_0t_Q)\ , \tag{2.11}$$

where $v_{\text{eff}}\psi_Q=t_Q\phi_Q$; i.e., t_Q is the amplitude due to the coupling to the Hilbert space of two or more pions, i.e, the Q_2 channel, and results from a solution of

$$(E-\mathcal{H}_{QQ})\psi_Q=0\ . \tag{2.12}$$

In Eq. (2.11) the effective Hamiltonian $\mathcal{H}_{PP}$ is given by

$$\mathcal{H}_{PP}=H_{PP}+H_{PQ}\frac{1}{E^{+}-\mathcal{H}_{QQ}}H_{QP}\ . \tag{2.13}$$

Hence by eliminating the spaces of zero pions (P-space) and two or more pions (Q_2-space), we have reformulated the equations as a scattering problem for the pion-nucleon system.

It is interesting to observe that had we instead eliminated the Q_1- and the Q_2-space in favor of the P-space, then the following equation results:

$$\left[E-H_{PP}-H_{PQ}\frac{1}{E-\mathcal{H}_{QQ}}H_{QP}\right]P\psi=0\ . \tag{2.14}$$

This eigenvalue problem will give us the baryon spectrum and since it includes the contribution from that part of the Hilbert space with one or more pions, the resultant baryon spectrum includes the meson correction to the baryon masses. This also has the effect of making the eigenvalues complex, which in effect gives the baryons a width for decay via meson emission. Comparing Eqs. (2.11) and (2.14) we observe that the operator that gives us the mass spectrum, including meson corrections, is present in the denominator of the second term on the right-hand side of Eq. (2.11). This implies that the values for the baryon masses correspond to poles of the pion-nucleon S matrix in the complex energy plane, which is what we expect. Here we note that in Eq. (2.14) the energy E is a nonlinear parameter that we need to determine self-consistently, and in this way determine the position of the S-matrix pole. Thus if we consider Eq. (2.14) as a set of homogeneous equations, then E is determined by the requirement that the determinant of the coefficients is zero. This value of E has to be determined separately for every pole in the S matrix.

Now, since H_{PP} is the Hamiltonian describing a baryon in the absence of coupling to the pion, its expectation value will be the bare mass of the baryon, $m^{(0)}$. This may incude any contribution from gluon exchange since that is not included in our starting Hamiltonian. The extra term in Eq. (2.14) includes the contribution due to the interaction with the pion, and is thus a correction to the bare baryon mass which is termed the self-energy $\Sigma(E)$. Hence we can rewrite Eqs. (2.11) and (2.14) as

$$\begin{aligned}\langle\phi|T|\phi\rangle&=\langle\phi|t_Q|\phi\rangle\\&\quad+\left\langle\psi_Q\left|H_{QP}\frac{1}{E^{+}-m^{(0)}-\Sigma(E)}H_{PQ}\right|\psi_Q\right\rangle\end{aligned} \tag{2.15}$$

and

$$[E-m^{(0)}-\Sigma(E^{+})]P\psi=0\ , \tag{2.16}$$

with

$$\Sigma(E)=H_{PQ}\frac{1}{E-\mathcal{H}_{QQ}}H_{QP}\ , \tag{2.17}$$

where $\mathcal{H}_{QQ}$ is a complex and energy-dependent operator defined in the π-B Hilbert space and includes the coupling to two or more pion intermediate states. In writing Eq. (2.15) we have made use of the fact that the distortion operator $(1+G_0t_Q)$ acting on a plane-wave pion-nucleon wave function ϕ_Q gives the scattering wave function ψ_Q. In this way we have established a one-to-one correspondence between the baryon spectrum, and the resonances observed in pion-nucleon scattering. In particular, the width of the resonance is the imaginary part of the energy E at which Eq. (2.16) is satisfied, while the baryon mass is the real part of this energy E. In the event that the Hilbert space of three-quark states admits more than one baryon with the same quantum number, then Eq. (2.16) becomes a matrix equation whose dimension is identical to the number of such states. This is, for example, the case in the P_{11} channel where we have the nucleon, and possibly the two states, corresponding to radially exciting one of the quarks in the baryon. These two states correspond to the [56] and the [70] representations of SU(6) (Ref. 13). Thus the problem of calculating the baryon spectrum has been reduced to a search for the solution of a nonlinear eigenvalue equation to be solved in the appropriate Reimann sheet of the complex energy plane. The equivalent π-N scattering problem is a solution of Eq. (2.8), which corresponds to scattering by the potential $\mathcal{V}$ given by

$$\mathcal{V}=H_{QP}\frac{1}{E^{+}-H_{PP}}H_{PQ}+v_{\text{eff}}\ , \tag{2.18}$$

which is the sum of two contributions. The first term is the result of coupling to the zero-pion Hilbert space, i.e., P-space, while the second term is the result of coupling to states with two or more pions, i.e., Q_2-space.

The above procedure for calculating $\Sigma(E)$ is guaranteed to satisfy two-body unitarity, and to that extent includes all decay modes involving single-pion final states, e.g., πN and $\pi\Delta$. To include the decay to two-pion final states, e.g., $\pi\pi N$ and ρN, we need to satisfy three-body unitarity. In that case the result for $\Sigma(E)$ has been derived[9] using the classification of diagrams according to their irreducibility, and the final result involves the solution of the πN-$\pi\pi N$ equations,[18] which are three-body-type equations.

A common procedure for calculating the baryon spectrum[13] involves linearizing the problem by taking E in $\Sigma(E)$ to be real, e.g., the bare mass $m^{(0)}$, and then calculating the eigenvalue of the real part of $\Sigma(E)$. This gives the mass of the baryon including pionic corrections. To get the width of that baryon we then make use of the resultant eigenvectors in conjunction with "Fermi's golden rule." To illustrate this we consider the case when $v_{\text{eff}}=0$, i.e., no coupling to the two-or-more-pion Hilbert space. We now can write the self-energy for real E as

$$\Sigma(E^{+})=H_{PQ}\frac{\mathcal{P}}{E-H_{QQ}}H_{QP}-i\pi H_{PQ}\delta(E-H_{QQ})H_{QP} \tag{2.19a}$$

$$\equiv\Delta m-\frac{i}{2}\Gamma\ , \tag{2.19b}$$

where the definition of Γ above is identical to Fermi's golden rule. In this way we have replaced a complex eigenvalue problem in the complex energy plane by a real eigenvalue problem on the real axis. The success of such an approximation depends to a large extent on the variation with energy of $\Sigma(E)$ as we move from the real axis to the position of the pole in the complex energy plane. This sensitivity is particularly important if $\Sigma(E)$ is a matrix with large complex off-diagonal elements. To see how this energy variation depends on the details of our model we need to explicitly write the real and imaginary parts of the self-energy for the case when $v_{\text{eff}}=0$. To make sure we are on the correct energy plane we need to deform our contour of integration in the k plane as the energy acquires a negative imaginary part: i.e., $E\to E_R-iE_I$ (see Fig. 1). The integral along the contour can now be written as an integral along the real axis, plus the residue at the pole in the complex k plane corresponding to $E-\epsilon(k)-\omega(k)=0$. This means that the self-energy is given by

$$\Sigma(E_R-iE_I)=\int_0^{\infty}dk\,k^2\frac{[u(k)]^2}{[E_R-E(k)]^2+E_I^2}[E-E(k)+iE_I]-2\pi ik_0\mu(k_0)[u(k_0)]^2\ , \tag{2.20}$$

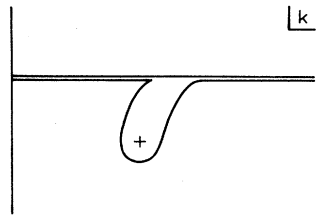

FIG. 1. The contour of integration in the k plane when the energy has a negative imaginary part.

where $E(k)=\varepsilon(k)+\omega(k)$, the reduced mass μ is given by

$$\mu(k)=\frac{\varepsilon(k)\omega(k)}{\varepsilon(k)+\omega(k)}\ ,$$

and k_0 is determined by the condition that

$$E(k_0)=E_R-iE_I\ .$$

In Eq. (2.20), $u(k)$ is the radial part of the coupling between the P-space and Q-space; i.e., H_{PQ}. We now observe that in the limit as $E_I\to 0$, the imaginary part of the integrand in Eq. (2.20) has a δ function that leads to a cancellation of half the contribution from the residue, the second term on the right-hand side of Eq. (2.20). On the other hand, for finite E_I, the imaginary part of the integrand has a Lorentzian distribution peaked about the momentum corresponding to the position of the pole, i.e., $\text{Re}[k_0]$. This implies that the imaginary part of the integral in Eq. (2.20), for a given value of k_0, will depend on the range of the form factor $u(k)$, and thus the radius of the bag. In particular, for a small bag radius, $u(k)$ is long range in momentum space and the integral is large. On the other hand, when the radius of the bag is small, the overlap between the form factor and Lorentzian is small, and the imaginary part of the integral is small.

To illustrate this we consider π-N scattering in the P_{33} channel, where the diagram that contributes most to the Δ width is shown in Fig. 2. The contribution to the width comes from two sources; one is the imaginary part of the integral in Eq. (2.20) and the other is the imaginary part arising from the residue. As one ventures into the complex plane, it is obvious that the imaginary part of the integral is always positive, while numerical studies have shown that the residue always has a negative imaginary part. Thus the two will cancel each other and the width then is determined by the relative magnitudes of these two terms.

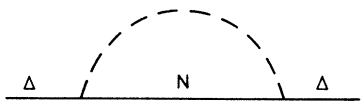

FIG. 2. The diagram that is included in the calculation of $\Sigma(E)$ for the P_{33} channel.

To examine the sensitivity of our result to the bag radius, we present in Fig. 3 the imaginary part of $\Sigma(E)$ as a function of the imaginary part of the energy for three different bag radii: $R=0.8$, 1.0, and 1.2 fm. Here we take $f_{\pi N\Delta}=2f_{\pi NN}$ and $f^2_{\pi NN}=0.08$. It is clear from Fig. 3 that as the bag radius is reduced there is more cancellation between the integral and the residue, and this cancellation increases as one moves into the complex plane. This suggests that the width we calculate on the real energy axis may have little resemblence to how far the pole of the S matrix is from the real axis. This is particularly the case for baryon resonances where the total widths are large. More important is the fact that the π-N amplitude, the experimentally observed quantity, reflects the result of the complex eigenvalue problem, i.e., the S-matrix pole, and not the result of the width as calculated on the real axis, i.e., Fermi's golden rule.

III. RESULTS

Having established the equivalence between the π-N scattering problem, Eq. (2.8), and the calculation of the baryon spectrum as an eigenvalue in the complex energy plane, Eq. (2.16), we proceed in this section to apply our formulation to the $J=\frac{1}{2}$, $T=\frac{1}{2}$ states in π-N scattering. The motivation for our choice of this channel is the fact that the π-N scattering calculation based on the CBM invariably predicts a very narrow $N^*(1440)$ resonance.[11] On the other hand, analyses based on calculating the mass and width of this resonance tend to give a width that is consistent with experiment.[13] Taking into consideration the result we presented in Fig. 3 for the $\Delta(1230)$, this apparent discrepancy between the two calculations may be due to the fact that the baryon mass has been calculated as a bound-state problem on the real energy axis. The other motivation for examining the Roper resonance, is the question of the existence of two possible Roper resonances very close to each other.[15] The model we consider admits two such states based on the [56] and [70] representation of SU(6).

The basic full model we consider for π-N scattering involves taking the Q_1-space to include $B=N$, Δ, [56], and [70]. This means that Eq. (2.8) could have as many as four coupled equations to solve. On the other hand, for our P-space, Eq. (2.16) can have as many as three equations with $B=N$, [56], and [70]. Finally, we have neglected the contribution of the Q_2-space by taking v_{eff} to be zero. The interaction Hamiltonian, in the present calculations, is taken from the CBM with pseudoscalar surface coupling. This means our Hamiltonian has three parameters. (i) The bare mass of the nucleon, $m_N^{(0)}$, which is adjusted so that the dressed mass as predicted by Eq. (2.16) is the physical nucleon mass $m_N=940$ MeV. (ii) For the Roper resonance we take the bare mass of the two states, the [56] and the [70], to be the same. This bare mass $m_R^{(0)}$ is then adjusted so that the real part of the energy of the lower resonance is 1440 MeV. (iii) The coupling of the pion to the quark is taken so that $f_\pi=93$ MeV. Finally, we take the bag radius to be 1.0 fm.

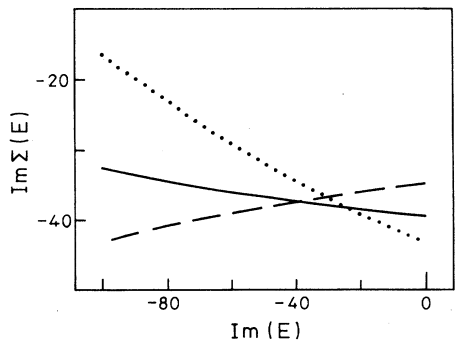

FIG. 3. The variation in the $\text{Im}\Sigma(E)$ as a function of $\text{Im}E$, keeping $\text{Re}E$ constant for three different bag radii R. The solid curve is for $R=1.0$ fm, the dashed line is for $R=1.2$ fm, while the dotted line is for $R=0.8$ fm.

In calculating the baryon spectrum using Eq. (2.16), we first observe that the matrix $M(E)\equiv m^{(0)}+\Sigma(E)$ is in general complex and energy dependent, and for the equation to have a solution the determinant of $[E-M(E)]$ must be zero. This reduces the problem of finding the poles of the S matrix in the complex E plane, to finding those energies for which $\det[E-M(E)]=0$. If this energy is real and less than $(m_\pi+m_N)$, then the position of the pole gives the nucleon mass, m_N. On the other hand, energies for which $\text{Re}(E)>(m_\pi+m_N)$ and can be approached from the real axis by taking the imaginary part of the energy to be less than zero correspond to resonances. In this case we expect two such resonances due to the fact that we have included radial excitation corresponding to the two representations of SU(6). The solution of Eq. (2.16) at the poles of the S matrix give us the components of the wave function of the resonances in terms of the N, [56], and [70] representations.

To begin with, we want to investigate the effect of calculating resonant poles when the energy is restricted to the real axis when one ventures into the complex energy plane. We initially look at the mixing between the [56] and [70] representations, and so truncate the P-space to include only these two states, while the Q_1-space has these as well as the nucleon and the delta. We also restrict our analysis to the case of $v_{\text{eff}}=0$. For this model we find the bare Roper mass, the only parameter in this case, to be $m_R^{(0)}=1557$ MeV, and the two resonance poles are at

$$E_1=(1440-16.5i)\text{ MeV}\,,\qquad E_2=(1526-65.1i)\text{ MeV}\,. \tag{3.1}$$

Here we note that lower-energy resonance has its main contribution from the [56] representation and has a relatively narrow width, while the second resonance, with main contribution from the [70] representation has a width that is comparable to experiment. This suggests that if we need to include the Roper as a radial excitation of a three-quark state, then it is essential that the [70] representation be also included, which has not always been the case.[11,12,16]

More interesting is the observation that these results

are in conflict with the work of Umland *et al.*[13] who carry out their calculation on the real axis using the same Lagrangian, the only difference between the two calculations being the absence of gluon exchange in our calculations, which they show to be small. To examine the origin of this difference we follow their procedure and diagonalize the real part of $M(E)$ by writing it as $U^T D(E) U$, where $D(E)$ is a diagonal matrix that gives the mass of the baryons. In this case we find that

$$D = \begin{bmatrix} 1421 & 0 \\ 0 & 1536 \end{bmatrix} . \tag{3.2}$$

We now use the matrix U, for $E = m_R^{(0)} = 1557$ MeV, to calculate the width of the two states as the diagonal elements of

$$U^T \mathrm{Im}[M(E)] U = \begin{bmatrix} -52 & 9 \\ 9 & -54 \end{bmatrix} . \tag{3.3}$$

Although this procedure gives baryon masses that are in reasonable agreement with the position of the poles of the S matrix, the resultant widths do not agree [compare Eq. (3.1) with Eqs. (3.2) and (3.3)]. The situation does not improve if we consider the eigenvalues of the complex matrix $M(E)$ which are given by

$$\begin{bmatrix} 1421-52i & 0 \\ 0 & 1536-54i \end{bmatrix} , \tag{3.4}$$

for $E = m_R^{(0)} = 1557$ MeV. It is interesting to note that on the real axis, the matrix which exactly diagonalizes $\mathrm{Re}[M(E)]$ also approximately diagonalizes $\mathrm{Im}[M(E)]$. The above results suggests that the calculation of baryon resonance widths as a real or complex eigenvalue problem on the real axis can give the wrong results if the widths are large, which is the case for most of the resonances observed in π-N scattering. This is mainly due to the fact that the $\Sigma(E)$ changes as we move from the real energy axis into the complex plane. This situation is similar to that of the Δ resonance considered in the last section. More interesting is the fact that the procedure of diagonalizing the $\mathrm{Re}[M(E)]$ also is not valid at the S-matrix pole even though it was a good approximation on the real axis. This is predominantly due to the fact that the imaginary nondiagonal elements of $M(E)$ become large. To illustrate this we consider first the eigenvalues of $M(E)$ for $E = (1440\text{-}16.5i)$, which is the position of the lower energy resonance. These are given by

$$\begin{bmatrix} 1440-16.5i & 0 \\ 0 & 1513-46i \end{bmatrix} . \tag{3.5}$$

Here we find that diagonalizing $M(E)$ at one pole gives the mass and width of that resonance, but not the position of the higher-energy resonance. Although we have two eigenvalues for $M(E)$, only one of them is a solution to Eq. (2.16). This is a result of the fact that $M(E)$ is energy dependent. On the other hand, the eigenvalues of the $\mathrm{Re}[M(E)]$ are given by

$$\begin{bmatrix} 1435 & 0 \\ 0 & 1519 \end{bmatrix} , \tag{3.6}$$

while

$$U^T \mathrm{Im}[M(E)] U = \begin{bmatrix} -18 & 22 \\ 22 & -44 \end{bmatrix} . \tag{3.7}$$

By comparing Eq. (3.5) with Eqs. (3.6) and (3.7), we observe that the matrix U which diagonalizes the $\mathrm{Re}[M(E)]$ does not diagonalize the $\mathrm{Im}[M(E)]$. Thus we may conclude that the source of the discrepancy between our results and those of Umland *et al.*[13] is the fact that they diagonalize a real matrix on the real energy axis, while we determine the poles of the S matrix. Finally, we note that in calculating the position of the S-matrix poles we are in fact determining two energies for which Eq. (2.16) has a solution, and these two solutions do not come from the diagonalization of a single matrix.

We now turn to π-N scattering in the P_{11} channel to see the correspondence between the resonance poles as calculated using Eq. (2.16) and the phase shifts. To get a more realistic description of π-N scattering in this channel, we need to extend our P-space to include the nucleon. This will give us the low-energy negative phase shifts that experiment predicts. We now have three parameters: the bare nucleon mass $m_N^{(0)}$, the bare Roper mass $m_R^{(0)}$, and the bare coupling constant. The bare masses are adjusted so that Eq. (2.16) gives the physical nucleon mass of 940 MeV and the mass of the lower-energy Roper at 1440 MeV. The coupling constants are determined by the CBM.

In Table I we present the values of the bare masses and the position of the S-matrix poles as determined by Eq. (2.16). Also included are the results of the position of the poles if we exclude from our P-space either the [56] or [70] representation. The surprising effect of including the nucleon is the reduction in the width of both Roper resonances. This is particularly the case with the resonance dominated by the [56] representation. A careful examination of Eq. (2.16) reveals that the reason for the reduction in width of the Roper is predominantly due to the stronger coupling between the nucleon and the [56] and [70] states, and can be attributed to the fact that $f_{\pi NN} > f_{\pi NR}$. In particular, the imaginary part of this coupling is large since there is no energy denominator to suppress this term. As a result the coupling between the nucleon and [56] is stronger than the coupling between the [56] and [70].

Since in this case one of the poles is close to the real energy axis, we can compare the result of the pole search with the results of taking the eigenvalues of the matrix $M(E)$ for $E = 1440$. This gives

$$D = \begin{bmatrix} 794.7-205.0i & 0 & 0 \\ 0 & 1440.6-3.3i & 0 \\ 0 & 0 & 1480.5-38.8i \end{bmatrix} , \tag{3.8}$$

with the bare masses as given in Table I. This clearly

TABLE I. The position of the S-matrix poles for different choices of channels in the P- and Q_1-spaces.

Truncation	Bare masses	Poles
P:N,[56],[70]	$m_N^{(0)}=1092$	(940,0)
Q_1:N,Δ,[56],[70]	$m_R^{(0)}=1524$	(1440,−2.8)
		(1473,−51.3)
P:N,[56]	$m_N^{(0)}=1087$	(940,0)
Q_1:N,Δ,[56]	$m_R^{(0)}=1517$	(1440,−7.4)
P:N,[70]	$m_N^{(0)}=1073$	(940,0)
Q_1:N,Δ,[70]	$m_R^{(0)}=1496$	(1440,−33.3)

suggests that for the narrow resonances, i.e., widths of the order of a few MeV's, the approximation of calculating the eigenvalues of $M(E)$ on the real energy axis is valid, but for the wider resonances, such as the higher-mass Roper resonance, this approximation can fail.

We now turn to the phase shifts for this model. In Fig. 4 we present the P_{11} phase shift as a function of the center-of-mass energy $E_{\text{c.m.}}$. Also included in the figure are the experimental phase shifts of Arndt *et al.*[14] As expected the phase shifts are small and negative at low energies, and they go through $\pi/2$ at an energy corresponding to the wider of the two Roper resonances. The effect of the narrow resonance at 1440 MeV is to produce a small bump in the phase shifts at this energy. To examine in more detail the bump in the phase shifts, we show, in Fig. 5, a magnified plot of the phase shifts, in the energy region of the resonance, which shows it smooth behavior. A similar behavior is found in the inelasticity η, see Figs. 6 and 7, in that the narrow resonance produces a sharp minimum observed under magnification in Fig. 7, while the higher mass resonance gives a broad dip in η. This small bump in the phase shifts gives an interesting signature when the Argand diagram is examined. In Fig. 8 we present a plot of the Im[f] versus the Re[f], where f is the π-N amplitude calculated in this model. Here we find that this narrow Roper resonance gives a small indent in the Argand diagram (see the magnified Argand plot in Fig. 9). As the width of this narrow resonance increases, this indent in the Argand diagram develops into a loop. On the other hand, the wider resonance corresponds to a change in the sign of Re[f].

In comparing our results with experiment in Figs. 4–9, we have demonstrated that on a qualitative level we have agreement with experiment to the extent that any conclusion drawn on the method of calculating the baryon resonances will hold in a more complete calculation. To get a better agreement with experiment we need to include more physics by including the cross diagram and possibly the contact diagram that results from the cloudy-bag model with volume coupling. Since the Roper is above the threshold for pion production, we need to include this threshold as well. These additional contributions have been shown to improve the agreement between theory and experiment.[18] However, as yet no calculations, including all these contributions, have been carried out to determine the position of the S-matrix poles in the complex energy plane. This is partly due to the complexity of any such analysis.

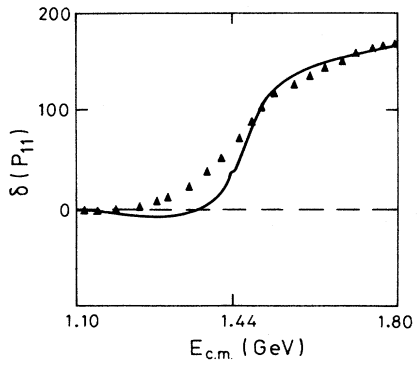

FIG. 4. The π-N phase shifts in the P_{11} channel. The P-space includes the N, [56], and [70]. The Q_1-space has N, Δ, [56], and [70]. The experimental data, solid triangles, are from Ref. 14.

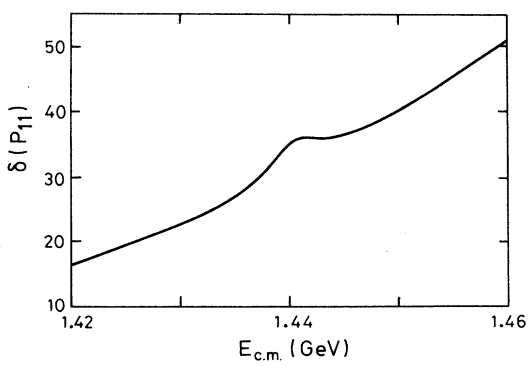

FIG. 5. The P_{11} phase shift in the region of the lower-energy Roper resonance (i.e., at 1440 MeV). This is a magnification of Fig. 4.

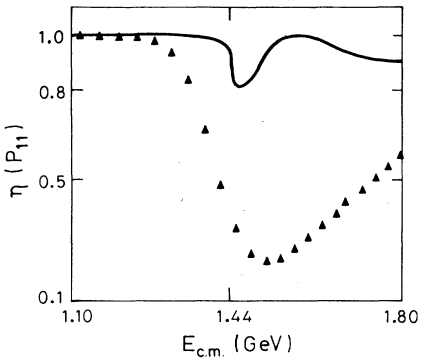

FIG. 6. The inelasicity η for π-N scattering in the P_{11} channel. The model is the same as that used to calculate the phase shifts in Fig. 4. The experimental data, solid triangles, are from Ref. 14.

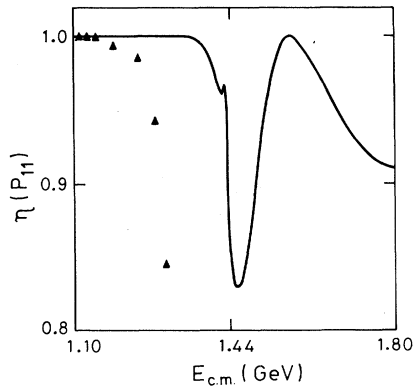

FIG. 7. A magnification of Fig. 6 to show the narrow dip due to the resonance at 1440 MeV.

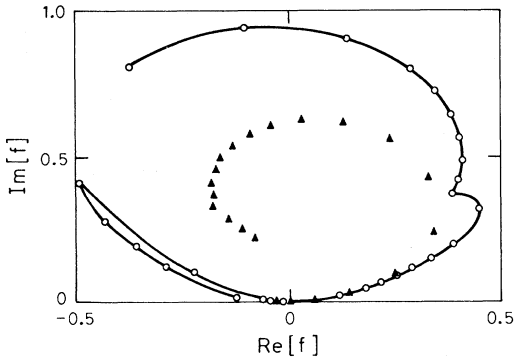

FIG. 8. The Argand diagram for the P_{11} amplitude. Included also are the amplitudes from the phase-shift analysis of Arndt *et al.* (Ref. 14).

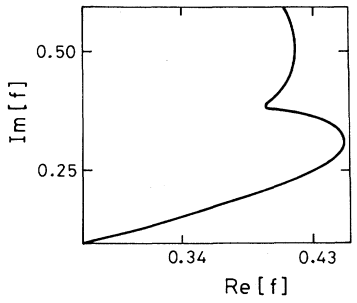

FIG. 9. The magnification of the Argand diagram in Fig. 8. The energy covered is identical to the energies considered in Fig. 5, i.e., between 1.42 and 1.46 GeV.

IV. CONCLUSIONS

The resonances observed in π-N scattering, with widths of the order of 100 MeV, have in recent years become the testing ground of quark models such as the chiral bag model. In the present analysis we have examined two methods of calculating the masses and widths of these baryon states. The first involved the solution of a complex eigenvalue problem in the complex energy plane. This procedure determines the position of the poles of the S matrix in the complex energy plane, and to that extent reflects the experimentally measured π-N amplitude. This procedure gives both the mass and width of a baryon resonance as the real and imaginary parts of the energy at which the S matrix has a pole. The second approach, often used for this problem is to consider the determination of the mass as a real eigenvalue problem on the real energy axis, i.e., a bound-state problem, and then use the resultant eigenstates to calculate the widths using Fermi's golden rule.

Taking as our basic Lagrangian that of the cloudy-bag model, we have shown that the second approach described above gives a poor approximation to the width if the S-matrix pole is far from the real energy axis. In particular, for the Roper resonance, we have found by taking both the [56] and [70] representations of SU(6) as a basis, that the coupling between these states is such that the second approach gives both resonances to have comparable width as previously reported by Umland *et al.*[13] On the other hand, a determination of the S-matrix poles gives one resonance a substantially smaller width than the second method, indicating the failure of the Fermi's golden rule for these resonances. Furthermore, this narrower resonance is mainly the [56] representation, suggesting that the [70] representation needs to be included in π-N scattering calculation, which has not been the case.[11,12,16] In addition, if we include the coupling of the [56] and [70] to the bare nucleon as a $(1s_{1/2})^3$ configuration, we find that both resonances are substantially reduced in width. This is the result of the strong coupling between the bare nucleon and the [56] and [70] states, as is a consequence of the fact that $f_{\pi NN} > f_{\pi NR}$, where R=[56] or [70]. These narrow resonances lead to small indents in the Argand diagram which are not observed in

the present phase-shift analysis. This suggests that either the present bag model gives a poor description of the Roper, e.g., the ratio of $f_{\pi NR}$ to $f_{\pi NN}$ is not given correctly by this simple bag model, or that there are other mechanisms not included that will give additional width. At this stage we know that the crossed and contact terms give additional attraction, and in fact their inclusion leads to good agreement between the bag model with volume coupling and experiment.[12] Finally, the present analysis resolved the apparent discrepancy between the calculation of the π-N scattering phase shift[11,12] and baryon spectroscopy[13] for the same Lagrangian.

ACKNOWLEDGMENTS

The authors would like to thank the Australian Research Council for their financial support.

[1]A. W. Thomas, Adv. Nucl. Phys. **13**, 1 (1984).
[2]D. J. Gross and F. Wilczek, Phys. Rev. Lett. **30**, 1343 (1973).
[3]A. De Rújula, H. Georgi, and S. L. Glashow, Phys. Rev. D **12**, 147 (1975).
[4]A. Chodos, R. L. Jaffe, K. Johnson, C. B. Thorn, and V. F. Weisskopf, Phys. Rev. D **9**, 3471 (1974); A. Chodos, R. L. Jaffe, K. Johnson, and C. B. Thorn, *ibid.* **10**, 2599 (1974); T. DeGrand, R. L. Jaffe, K. Johnson, and J. Kiskis, *ibid.* **12**, 2060 (1975).
[5]H. Pagels, Phys. Rep. **16C**, 219 (1975); B. W. Lee, *Chiral Dynamics* (Gordon and Breach, New York, 1968).
[6]A. Chodos and C. B. Thorn, Phys. Rev. D **12**, 2733 (1975).
[7]G. E. Brown and M. Rho, Phys. Lett. **82B**, 177 (1979).
[8]S. Théberge, A. W. Thomas, and G. A. Miller, Phys. Rev. **22**, 2838 (1980); **23**, 2106(E) (1981); A. W. Thomas, S. Théberge, and G. A. Miller, *ibid.* **24**, 216 (1981); S. Théberge, Ph.D. thesis, University of British Columbia, 1982.
[9]I. R. Afnan and B. C. Pearce, Phys. Rev. C **35**, 737 (1987).
[10]H. Feshbach, Ann. Phys. (N.Y.) **19**, 287 (1962).
[11]E. A. Veit, B. K. Jennings, and A. W. Thomas, Phys. Rev. D **33**, 1859 (1986).
[12]B. C. Pearce and I. R. Afnan, Phys. Rev. C **34**, 991 (1986).
[13]E. Umland, I. Duck, and W. von Witsche, Phys. Rev. D **27**, 2678 (1983).
[14]R. A. Arndt, J. M. Ford, and L. D. Roper, Phys. Rev. D **32**, 1085 (1985).
[15]A. Mokhtari *et al.*, Phys. Rev. D **33**, 296 (1986).
[16]A. S. Rinat, Nucl. Phys. **A377**, 341 (1982).
[17]I. R. Afnan and A. T. Stelbovics, Phys. Rev. C **23**, 1384 (1981); M. L. Goldberg and K. M. Watson, *Collision Theory* (Wiley, New York, 1964).
[18]B. C. Pearce and I. R. Afnan, Phys. Rev. C **40**, 220 (1989).